This is a peer-reviewed, accepted author manuscript of the following conference paper: Li, T, Zhang, M, Yu, S-R & Yuan, Z-M 2022, Real-time control of WECs based on NAR, NARX and LSTM artificial neural network. in JS Chung, I Buzin, H Kawai, et al. (eds), *The Proceedings of The Thirty-second (2022) International Ocean and Polar Engineering Conference.* vol. 1, International Society of Offshore and Polar Engineers, Cupertino, CA, pp. 359-367, The Thirty-second (2022) International Ocean and Polar Engineering Conference, Shanghai, China, 5/06/22.

Real-time Control of WECs Based on NAR,NARX and LSTM Artificial Neural Network

Tuo Li[1], Ming Zhang[2], Shuang-Rui Yu[2], Zhi-Ming Yuan[1,2]

[1] School of Naval Architecture and Ocean Engineering, Jiangsu University of Science and Technology, Zhenjiang Jiangsu, China

[2] Department of Naval Architecture, Ocean and Marine Engineering, University of Strathclyde, Glasgow, UK

ABSTRACT

In this study, we aim to improve WECs' performance for maximizing energy absorption through a sub-optimal method of phase control by latching is applied to the device.The forecasting of future wave force is required for the optimal control command deducted.An artificial neural network, namely LSTM (Long Short-Term Memory) is proposed to accurately predict the short-term wave force. The hydrodynamic properties of a point absorber is analyzed based on the 3D potential flow theory in frequency-domain. Cummin's equation and a 4th-order state-space model are used to efficiently represent the hydrodynamic behavior of the WEC under irregular waves in time-domain.The Nonlinear Autoregressive artificial neural network(NAR-ANN) and NARx network are used to verify the method proposed in this paper. The simulation results show that the mean square error value, root mean square error value and R^2 value based on the LSTM prediction model are better than those of the NAR prediction model. The prediction performance of LSTM is more suitable for processing the time series.

KEY WORDS: wave force prediction, latching control, wave energy converter(WEC), LSTM, NAR-ANN, NARx.

INTRODUCTION

Wave energy is a kind of marine renewable energy. It is regarded as a forward-looking solution for sustainable power generation because of its high power density, high stability, good economic benefits and energy flow without intermission.Furthermore,the total exploitable amount is the same as the power consumption. A mainstream Wave energy converters (WECs) is the Oscillating Buoy(OB).To lower the levelized cost of energy (LCOE), a real-time latching control methods is being investigated. The latching control was first introduced by Budal and Falnes (Budal, 1980). Power absorption is achieved by locking and releasing the buoy alternately to keep the phase of WEC align with the wave excitation force. Babarit and Clement (Babarit, 2006) assessed the power extraction of an oscillating-body WEC with latching control. Previous studies focus on the optimal control, which assumed that the coming wave force was already known. But real-time latching control is result in non-causal transfer functions, so it make sense only if future wave force is known. Meanwhile, the information of future force is difficult to measure directly in real sea state. Falnes(Falnes,1995)explained the relation between wave elevation and wave excitation force is a non-linear dynamic system. Model predictive control (MPC) is a method that solve a series of successive, small time horizon, optimal control problems(Tom,2016) which requires the prediction of future wave force.The accuracy of the model of the body dynamics strongly affect the performance of real-time control methods (Anderlini, 2017).So it is necessary that build a prediction model as accurate as possible. A good prediction model includes not only suitable artificial neural networks but also MPC parameters match with the wave force prediction model. Truong(Truong,2011) has developed a wave force prediction model based on modified grey model MGM(1,1) for real-time control. ANN has applied to predict MPC wave force to improve power efficiency of a heaving point absorber WEC by Li(Li,2018). The time series of the elevation and wave excitation force have successfully predicted by using a LSTM-NARX model to achieve more accurate WECs real-time control by Zhang(Zhang,2020), the LSTM network is used to predict wave elevation and wave excitation force only by output data and the NARX-ANN is used to predict wave elevation by input and output.

In section 2, a numerical time-domain model of heaving point absorber is built and expressed by state-space equation. In section 3, a real-time latching control algorithm based on MPC is presented and give a more insightful understanding of chosen MPC parameters. In section 4, a simulation is conducted based on chosen WEC and MPC parameters. The motion response of floater suggested by frequency-domain hydrodynamic analysis programme WADAM produced by DNV-GL is used to verify the WEC dynamic model. The prediction difference between NAR and LSTM is presented by different value. The simulation results that the MPC and prediction model parameters.

DYNAMIC MODEL

According to the difference in working principle, WEC can be divided

into the following categories. Oscillating water column (OWC), overtopping and oscillating buoy (OB). Most offshore WEC devices belong to OB, which are located in deep water, with high energy flow density and can exploit more abundant wave energy resources. The research environment of this study is located in the deep ocean, using offshore oscillating buoy wave energy conversion device, and using direct-drive generators. Its energy conversion mechanism is to generate energy through the relative motion of a floater subjected to wave loads and the substrate fixed on the seabed. Assuming that the fluid is an incompressible irrotational ideal fluid, the mass of the buoy body dimensions is large and the amplitudes of oscillation are quite small. So the linear wave theory is applicable for wave-structure interaction analysis.

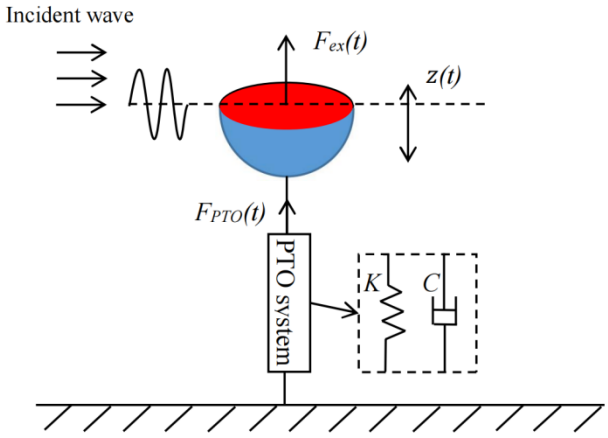

Fig. 1 Heaving buoy WEC.

As shown in Fig.1 , the floater is a hemisphere constrained in heave only, the power take-off(PTO) system is a mechanical oscillation system which can be modelled by spring and damping terms. Following the Newton's second law, the PTO system force analysis is shown in Eq.(1).

$$m\ddot{z}(t) = F(t) - F_{\mathrm{R}}(t) - F_S(t) \tag{1}$$

Here $F(t)$ is assumed external force, $F_R(t) = C\dot{z}(t)$is damping force, $F_S(t) = Kz(t)$is restoring force. So the stiffness coefficient K and damping coefficient C are employed to represent the PTO force in this study. Consequently, the PTO system can be regarded as a damping-spring system.Vicente(Vicente,2013) showed that the typical stiffness of a PTO system is around 10% of the hydrostatic coefficient, so there $K = 0.1\rho g\pi R^2$ is adopted in this study. The damping coefficient C which maximizes energy absorption efficiency is adopted the same as that in the study(Li,2018) because the model parameters are consistent. In each load case, the amplitude of the incident regular wave is 1 m.As shown, the energy conversion is maximized at $\mathrm{C} = 8.14 \times 10^5 \mathrm{kg/s}$. The power for incident regular wave is as Eq.(2).

$$P = \frac{\rho g^2 A^2 R}{2\omega} \tag{2}$$

The power for incident irregular wave is as Eq.(3).

$$P = \frac{\rho g^2 H_s^2 T_p R}{32\pi} \tag{3}$$

Then the average power P extracted by PTO over the interval $[0,T]$ is given by Eq.(4).

$$\hat{P} = \frac{1}{T}\int_0^T C \cdot \dot{z}(\tau)d\tau \tag{4}$$

In the same way, the equation of motion for oscillating WEC is expressed by Eq.(5).

$$m\ddot{z} = F_{ex} - F_{\mathrm{R}} - F_S - F_{PTO} \tag{5}$$

Where $m\ddot{z}$ is the inertial force. F_{ex} is the excitation force included diffraction force and Froude-Krylov force. In this study, since the buoy is quite small compared to the incoming wavelength, diffraction force is neglected. F_R is the radiation force which is decomposed into inertia force and damping force. F_S is the restoring force which is the difference between gravity force and buoyancy force caused by hydrostatic press. F_{PTO} is the force provided by the PTO.

According to the linear wave theory, the irregular wave elevations are formed by the superposition of a set of linear regular waves with different amplitudes, different frequencies and the random phases of regular wave. So the irregular wave elevation is expressed by Eq.(6).

$$\zeta(t) = \mathrm{Re}\left[\sum_{j=1}^{N} A_j e^{i(\omega_j t + \phi_j)}\right] \tag{6}$$

Where A_j ,ω_j ,ϕ_j are wave amplitude, the frequency and the phase. In this study, we focuses only on amplitude response so it uses the real part of the argument. For irregular wave the A_j is obtained by Eq.(7). For regular wave, the A is 1m which is the unit amplitude refers to the vertical distance from water surface to the crest or the trough in Eq.(11).

$$A_j = \sqrt{2S(\omega)\Delta\omega} \tag{7}$$

When the wave develops to a certain stage, its wave energy basically remains at a certain value, so the wave energy spectrum in a specific sea area has a certain form.$S(\omega)$ is wave spectral density function are given mannually. P-M wave spectrum is used to compute this time histories of the wave excitation force in this study and the formula is as follow in Eq.(8).

$$S(\omega) = \frac{0.78}{\omega^5}\exp\left(-\frac{3.11}{\omega^4 H_s^2}\right) \tag{8}$$

response amplitude operators(RAOs) is the transfer function in frequency domain which stand for the effect of sea state on floating body in water. It is a representative advantage of linear wave theory. There exists two types RAOs $H_{ex}(\omega)$ and $H(\omega)$in this study. $H_{ex}(\omega)$ is the transfer function which can be calculated by Eq.(9) (Falnes,1995)

for the wave excitation force and wave elevation.

$$H_{\mathrm{ex}}(\omega)=\frac{1}{2}\left(\frac{2g^3\rho B(\omega)}{\omega^3}\right)^{0.5} \tag{9}$$

Where $B(\omega)$ is the damping coefficient. The added mass and damping coefficient are the hydrodynamic forces and moments of rigid body in harmonic motion. A.Hulme(Hulme,1982) has derived the frequency-domain hydrodynamic coefficients(added mass and damping coefficients) with the periodic motions of a floating hemi-sphere by an empirical formula. The hydrodynamic coefficients in frequency domain are obtained by buoy's parameters and wave number given by the positive root of the dispersion relationship $\omega^2/g = ktanh(kh)$.

$H(\omega)$ is the ratio of buoy motion response and the response which shown below is the displacement to unit wave amplitude($A = 1m$) as showed in Eq.(10).

$$\mathrm{Z}(\omega)=AH(\omega) \tag{10}$$

In order to obtain RAO curve $H(\omega)$ in Eq.(10) in a given frequency range, the motion response $Z(\omega)$ needs to be obtained first by calculating the state-space equation by Runge-Kutta method and it will be mentioned in the next section. It represents the displacement after stabilization under the regular incident waves at each single frequency.

When no control is applied, WEC is a linear system. Then the wave analysis by diffraction and Morison theory(WADAM) is applicable to analyze the interaction between structure and wave. In this study, the transfer function under regular waves is obtained by WADAM and the excitation force under regular waves is calculated by Eq.(11).The irregular wave representation of the excitation force is given by Eq. (12).However, the wave excitation force under irreugular wave is obtained directly by SIMA produced by DNV-GL in this study.

$$F_{ex}(t)=AH_{ex}(\omega_{\mathrm{r}})\sin(\omega_r t) \tag{11}$$

$$F_{ex}(t)=\mathrm{Re}\left[\sum_{j=1}^{N}A_j H_{ex}(\omega_j)e^{i(\omega_j t+\phi_j)}\right] \tag{12}$$

Where $H_{ex}(\omega_r)$ is the magnitude of the frequency-domain excitation force for a given frequency ω_r. The excitation force is very important for the following time-domain motion equation of the floater deducted. The frequency-domain analysis above help clearly describe dynamic model of WEC, while the real sea state is nonlinear rather than linear. So we have to convert the frequency-domain model to the time-domain. The radiation force is caused by motion of floater as shown in Eq.(13), and Eq.(14) is deduced by conducting Fourier inversion on it.

$$F_R(\omega)=\omega^2 m_\infty(\omega)z(\omega)-V(\omega)B(\omega) \tag{13}$$

$$F_R(t)=m_\infty\ddot{z}(t)+\int_0^{\tau}h(t-\tau)\dot{z}(\tau)d\tau \tag{14}$$

$$h(t)=\frac{2}{\pi}\int_0^{\infty}B(\omega)\cos(\omega t)d\omega=\frac{2}{\pi}\int_0^{\infty}\frac{m_r(\omega)}{\omega}\sin(\omega t)d\omega \tag{15}$$

Where m_∞ is added mass when the frequency tends to infinity and $h(t)$ is time retardation function or sometimes impluse response function which represents the WEC memory effect. It can be calculated by added mass or damping coefficient as Eq.(15). The F_S is the restoring force can be obtained from the following foumula Eq.(16).

$$F_S(t)=mg-\rho g v=\rho g A_w z(t) \tag{16}$$

Where A_w is waterplane area, $z(t)$ is the displacement of buoy in heave.

REAL-TIME CONTROL

Latching Control

Mentioned in the previous section, the oscillating buoy heave with the wave to drive the PTO system to convert the kinetic energy into electric energy. However, there exists some serious problem if control is not applied, such as the efficiency of floater is unsatisfactory, the device will be damaged due to excessive amplitude, speed, power and so on. According to the difference in control strategies, it can be divided into the following two categories. In phase control and amplitude control, the former is more common. The energy absorption maximized when oscillating velocity in phase with the excitation forces. Phase control can be achieved by adjusting the resonant frequency of PTO device. The latching control used in this study belongs to so-called 'bang-bang control'. It helps the kinetic energy not to be dissipated by the wave forces. The external latching force F_c is defined as Eq.(17). Since the wave is random, in order to make the buoy's speed in phase with the excitation force, the future change of excitation force must be known before latching control be taken to change the speed of the buoy by changing the PTO force. Therefore, the system is non-causal. If the future wave forces are completely known, the optimal control can be achieved.

$$F_{\mathrm{c}}(t)=-cu\dot{z}(t) \tag{17}$$

Where c is a very large damping coefficient and $c = 80(m + m_\infty)$ is employed as in A.Babarit's study(A,Babarit,2006). u is the binary control variable with $u = 1$ then latching is applied and $u = 0$ when it is not. From all above, Eq.(2) can be expanded as Eq.(18) :

$$\begin{aligned} &m_\infty\ddot{z}(t)+\int_0^{\tau}h(t-\tau)\dot{z}(\tau)d\tau+\rho g\pi r^2 z(t)\\ &=F_{ex}-(C+cu)\dot{z}(t)-Kz(t) \end{aligned} \tag{18}$$

State-space Model

The simulation of time-domain model mainly lies in the realization of convolution term(Cummin,1962). In this study, the state-space equation

is used to approximate the convolution term due to its contribution to improving computation speed to solve Eq.(18) out . The state-space representation is a mathematical model of dynamic system. As a group of input included uncontrollable input F_{ex} and controllable input F_{PTO}, output included buoy's displacement and velocity, state variables , it is related by a first-order
differential equation. In this study, 4th-order-state-space representation is defined as:

$$\dot{u}(t)=\vec{A}u(t)+\vec{B}x(t) \quad , \quad \int_0^\tau h(t-\tau)\dot{z}(\tau)d\tau=\vec{C}u(t) \tag{19}$$

Where $u(t)$ is the state vector with dimension 4×1,$x(t)$ is the input with dimension 4×1 and $\vec{A},\vec{B},\vec{C}$ are the coefficient matrix which are determined by a system identification process. The convolution term represents the output. The WEC motion can be described as Eq.(20) by inserting Eq.(19) into Eq(18).

$$\dot{\boldsymbol{x}}=\boldsymbol{W}\boldsymbol{x}+\boldsymbol{Z} \tag{20}$$

Where

$$\boldsymbol{x}=\begin{bmatrix} z \\ \dot{z} \\ \boldsymbol{u} \end{bmatrix} \quad , \quad \boldsymbol{Z}=\begin{bmatrix} 0 \\ \dfrac{F_{ex}}{m+m_\infty} \\ \boldsymbol{0} \end{bmatrix}$$

$$\mathbf{W}=\begin{bmatrix} 0 & 1 & 0 \\ -\dfrac{\rho g\pi r^2+K}{m+m_\infty} & -\dfrac{C+c\beta}{m+m_\infty} & -\dfrac{\vec{\mathbf{C}}}{m+m_\infty} \\ 0 & \vec{\mathbf{B}} & \vec{\mathbf{A}} \end{bmatrix} \tag{21}$$

Eq.(21) is a first order differential equation which is solved by the 4th order Runge-Kutta method. The Hamiltonian is defined as two parts in Eq.(22).

$$\hat{H}=C\dot{z}^2+\boldsymbol{\lambda}\cdot(\boldsymbol{W}\boldsymbol{x}+\boldsymbol{Z}) \tag{22}$$

Where $C\dot{z}^2$ is objective function correspongding to the P in Eq.(4). And $\boldsymbol{\lambda}(\boldsymbol{W}\cdot x+\boldsymbol{Z})$ is corresponding to the state-space equations. The $\boldsymbol{x}$ is the state vector with dimension 6×1. The $\boldsymbol{\lambda}$ is the adjoint variable with dimension 1×6, which can be obtained by adjoint equation as Eq.(23) based on Pontragyin's maximum principle(PMP) .

$$\dot{\boldsymbol{\lambda}}_{\boldsymbol{i}}=-\frac{\partial H}{\partial \boldsymbol{x}_{\boldsymbol{i}}} \tag{23}$$

Integrating the equations above we can get Eq. (24).

$$\dot{\lambda}_1=\lambda_2\frac{\rho g\pi r^2+K}{m+m_\infty}$$

$$\dot{\lambda}_2=-2C\dot{z}-\lambda_1+\lambda_2\frac{C+c\beta}{m+m_\infty}-\sum_{i=1}^{n}\left(\lambda_{i+2}B_i\right)$$

$$\dot{\lambda}_{1+2}=\frac{\lambda_2 C_i}{m+m_\infty}-\sum_{j=1}^{n}\left(\lambda_{i+2}A_{ji}\right) \tag{24}$$

Zhong and Yeung(Zhong, 2017) use the quadratic programming (QP) formula to derive the control command. Quadratic programming refers to the optimization problem with quadratic objective function and constrained conditon. In general, the problem of maximizing energy absorbed under constraints can be regarded as an optimization problem for solving quadratic programming, which can ensure the existence of solutions. The application of PMP means that the optimal command time series u is the one that maximizes the Hamiltonian at each time step in [0. T].Then, the control command is derived as Eq.(25).

$$\beta=\begin{cases} 1 & \lambda_2 c\dot{z}<0 \\ 0 & otherwise \end{cases} \tag{25}$$

To get the control command time series from Eq.(25),we integrated Eq.(20) from t = 0 to t = T with the initial condition $\boldsymbol{Z}(0)=0$ to obtain the motion $\boldsymbol{Z}$ without latching control. Then Eq.(24) is integrated from t = T to t = 0 to obtain the adjoint variable λ. Finally, repeat the iteration process until the calculation converges. Henriques (Henriques, 2016) use the control command sequence derived at previous time step at the current time step, and execute the code within the iteration only once in order to ensure that each control does not affect each other and the prediction and optimization will be carried out again according to the new state at the next time step.

Model Predictive Control

The model predictive control(MPC) is the basic idea of real-time control strategy. The main difference in this study between MPC and other control methods is that it considers the effect of control quantity on the future state, which is realized by rolling optimization.Generally speaking, the optimal control needs to be optimized in the entire time domain, so as to ensure the optimality.However, since the wave force is unknown, we can only achieve sub-optimal control by forecasting the wave forces over a short interval $[t_i, t_i+p]$ from which the optimal control command is obtained under specific constraints. Subsequently, apply the command into the next time step $[t_{i+1}, t_{i+1}+p]$. This means that the optimization process is not carried out offline, but repeatedly online. This process belongs to closed-loop optimization.
The choice of MPC parameters will affect the optimization effect, optimization time and prediction error in each time step. The input of model predictive control is the predicted wave force in the future, so the selection of its parameters will also affect the maximization of time-averaged absorbed power. As shown below, wave excitation force can only be predicted within a certain prediction horizon. the predictive horizon Δt is 3.0s in this study, and the time step dt is 0.01s. Therefore, 300 future wave force data points are predicted over the prediction horizon.

PREDICTION MODEL

In this section, three methods, based on Deep Learning Dynamic Neural Network(NAR, NARX, LSTM) applied to forecast short-term wave excitation force in order to evaluate their adequacy, accuracy and reliable horizon. In contrast to static neural networks, dynamic neural networks are characterized by the presence of feedback or delay. And the main application of dynamic neural network is the prediction of time series. The dynamic neural network can be classified into two categories: feed-forward and recurrent and the recurrent (also known as memory Neural network) is mainly used in this study. For the prediction model in this study, the inputs are the wave elevation information in the past and the outputs are the wave excitation forces over the prediction horizon $[t_i, t_i + p]$.

The prediction model has several points to pay attention to:

a) The number of hidden layers. A hidden layer is required only if the data is non-linear separated. Giorgi(Giorgi, 2015) has shown the nonlinear relation between incident wave and excitation force. The deeper the number of layers, the stronger the ability to fit the nonlinear relation in theory. However, in fact, the deeper layers may bring the problem of overfitting, but also increase the difficulty of training and make the model difficult to converge. In this study, a two hidden layers prediction model is used.

b) The number of neurons for each layer. Each layer has the neurons to receive and send signals. In like wise, too few neurons in the hidden layer will lead to underfitting, while too many neurons will lead to overfitting. In general we take the same number of neurons for all hidden layers. In this study, a single hidden layers prediction model is confirmed by adjusting the number of layers.

c) The appropriate number of delay. The delay means the number of raw data n which are used for prediction in each time step. It also can be described as the length of history data. For example, the time step is 0.01s, the delay is $n = 10$, which means that the time length of history data is 0.1s backwards.

To calibrate the optimal number of hidden layers, neurons per layer, delay for NAR and NARX model. Several tests have performed range from 1 to 3 hidden layer and 1 to 20 neurons. It is worth mentioning that increase the number of hidden layer is more helpful to enhance the predictive model ability than simply increasing the number of neurons.

Data pre-process

Because different evaluation indicators often have different dimensions and ranges, this situation will have a bad effect on the results of data analysis. In order to eliminate the dimensional impact between indicators in training neural network, it is necessary to date pre-process which named normalization in this study in original data. It help find the optimal solution by gradient descent method faster and improve the calculation progress. Min-MaxNormalization is used in this study as Eq.(24) which is a linear transformation of the raw data. The data is in the range of $[0, 1]$ after the normalization process and can be compared together.

$$y^* = \frac{y - y_{min}}{y_{max} - y_{min}} \tag{26}$$

NAR-ANN Model

Non-linear Autoregresive artificial neural network model is an special dynamic neural network based on back propagation algorithm which can deal with time series non-linear problem. NAR model is used when it only have the output data of time series such as wave excitation force exported by SIMA.The NAR model in which the current output is only described as a linear combination of previous output of the time series.

$$y(t) = f\left(y(t-1), y(t-2), \cdots, y(t-n)\right) \tag{27}$$

Where $y(t)$ is the output, $y(t-1), y(t-2), \cdots, y(t-n)$are the past wave excitation force value of the time series and the n is the number of past output called delay used in the NAR model. f is the nonlinear function obtained by network. Because the output weight of each time step is different, the outputs are not simply added.

NAR prediction model is divided into two parts: train and prediction. Open-loop network is used to train and validate and it is an one-step-ahead prediction network as shown in Fig. 2.

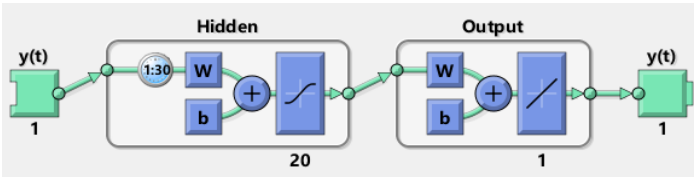

Fig. 2 The NAR-ANN open-loop network (From:MATLAB)

Closed-loop network is used to make multi-step prediciton as shown in Fig. 3.

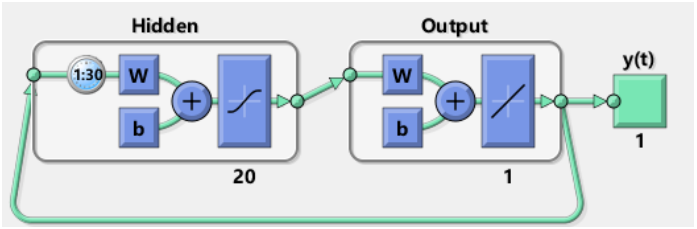

Fig. 3 The NAR-ANN closed-loop network (From:MATLAB)

The specific training and prediction process is as follows: First, input the wave excitation force data of the first n time steps. Then, replaces the data of the first time step with the first prediction output as the feedback input and continue to output the next prediction result through the close-loop network. So multi-step prediction can be implemented forward by gradually replacing the actual points in input regressor with predicted points. And the iterative times are called prediction horizon Δt as shown in Fig. 4. By predicting a little distance each time, it is nested into a large cycle for complete prediction.

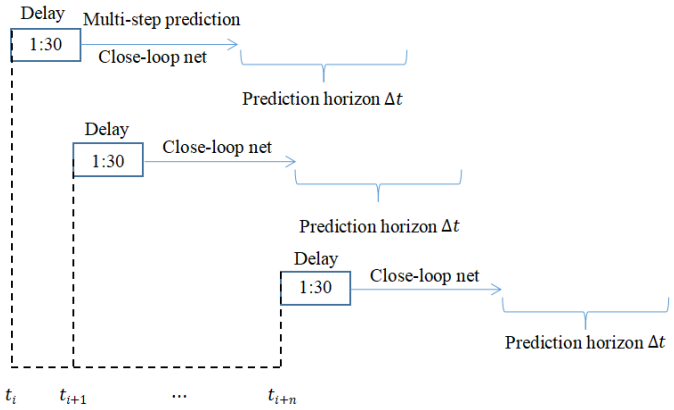

Fig. 4 Multi-step prediction application

In the validation of NAR neural network, the prediction results are in good agreement with the sample values. However, it cannot be said that this prediction model is good enough, because even a poor model model will perform similar to it. The reason is that the relationship between the two values in each time step is only a one-step prediction through open-loop network, and there is no connection between each time step.

Interpolation strategy application

Due to the shortcomings of the prediction method itself, the prediction results will accumulate the error. This determines that the number of prediciton steps called prediction horizon Δt is very limited. As shown in Fig. 5, only the prediction data of the first 0.3s is relatively accurate. And the longer the prediction steps are, the greater the error will be. But in fact, we can't take a quite small value in the prediction horizon Δt to obtain the more accurate prediction results. Because in the real-time control strategy, we use the optimal control theory to obtain the control sequence of wave force in the next time step and it need a quite long prediction horizon to get this control command. In order to give consideration to the effect of prediction and control, use the interpolation strategy to expand the number of forecasts. The strategy is implemented by uniform partition the delay vector when the neural network is trained and then interpolate the divided prediction results.

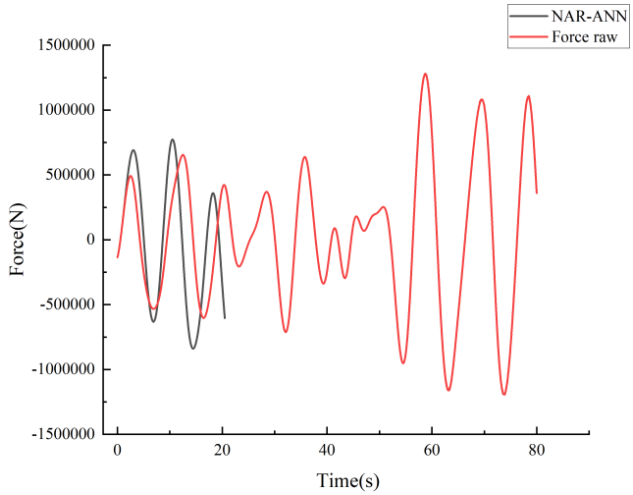

Fig. 5 Comparison of NAR-ANN predicted data and raw force data

As shown in Fig. 6 the prediction horizon Δt is longer than before. It meets the requirements of both prediction and control, so it determined as $\Delta t = 3s$ in this paper.

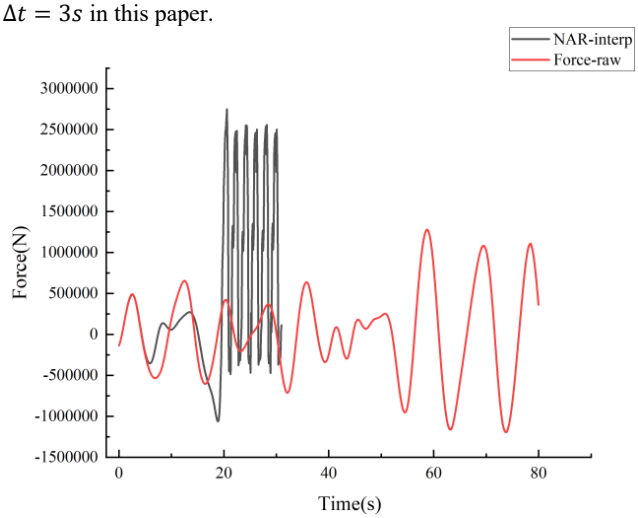

Fig. 6 Comparison of NAR-ANN interpolated predicted data and raw force

NARX Model

The Nonlinear Autoregressive model with exogenous input (NARX) added one or more exogenous covariate based on the NAR. Only the time history of the output is used for the NAR model and both input and output data are used for the NARX model. And the input data is equivalent to an auxiliary input which can improve accuracy by predicting the input first and then predicting the output. In this study, the history wave elevation is regarded as the exogenous variable input, and the history wave excitation force is regarded as the output. The future excitation force prediction is realized by inputting the future wave elevation.

$$y(t)=f\left(y(t-1),\ y(t-2),\cdots,\ y(t-n_y),\right.$$
$$\left.u(t),\ u(t-1),\ldots,\ u(t-n_u)\right) \tag{28}$$

Where $u(t)$ is the input and $y(t)$ is the output as NAR, the n_y is the number of past output called delay used in the NAR model.

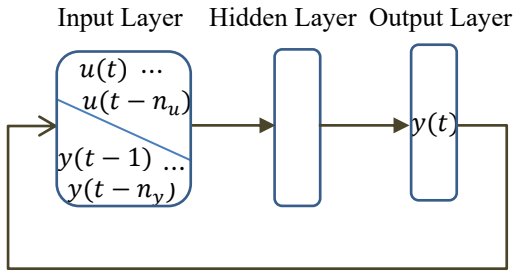

Fig. 7 Structure model of NARX neural network

As shown in Fig. 7, a NARX-ANN with a single hidden layers has been used in in this study. According to the analysis of Autocorrelation, the parameter of delay n=10 can be conducted. And it is very important to data pre-process that wave elevation and wave excitation force are in different order of magnitude. If data pre-process is not taken, the autocorrelation of error will be very large. So in NARX model, data pre-process and interpolation are combined use.

The number of neurons per hidden layer is estimated according to the following heuristics:

$$N_2=\sqrt{N_1+m+1}+a \tag{29}$$

Where N_1 is number of input neuron, m is number of output neuron, a can be chosen in 1 to 10. Generally, the neurons N_2 of each hidden layercan be taken as the same.

Table 1. Parameters applied in NAR and NARX prediction model

Parameters	Value
Layer	3
Neurons per layer	25
Delay	10
Cost function	RMSE
Learning rate	0.001
Activation function	Sigmoid
Time step	0.01s
Training set ratio	70%
Test set ratio	15%

LSTM Model

However, in the process of BP back propagation, it is necessary to take the derivative of the activation function, in which gradient explosion and gradient vanish will occur. Hochreiter first proposed LSTM in 1997. Compared to NAR and NARX, LSTM is a special recurrent neural network which has the inner loop and be able to solve the problem of long-term dependencies and the network state is updated in real-time.And instead of neurons, LSTM networks have memory unit that are connected through layers. It is characterized by the new added cell state c in hidden layer which can save long-term status. The transmission of LSTM memory unit is shown as Fig. 8.

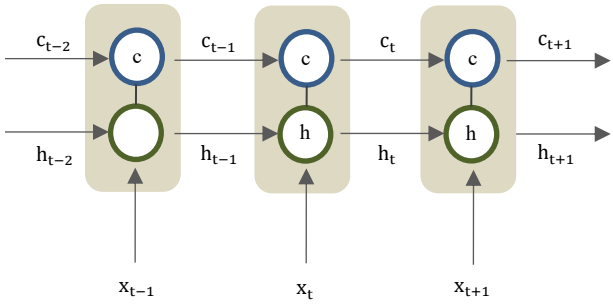

Fig. 8 The transmission in LSTM memory unit

The neuron of LSTM transmits two types of information:cell state c and hidden state h forward in time. In my opinion, cell state likes a highway, only the past information can transmit in it. But the hidden state like a ordinary road and current information mainly transmit in it. To solve the accumulated error, it has two methods to solve the problem of error accumulation. The first is to use the observed value instead of the predicted value to predict the next one, and its external network state is updated in real time. Three types of gates are used to control both the cell state and the hidden state of the layer. The detailed description between gates (input gate, output gate, forget gate) and the corresponding architecture which is the internal structure in the figure can be found in Zhang(2020). Because the feature extraction ability of LSTM is very strong, the three-Layers structure is generally enough.

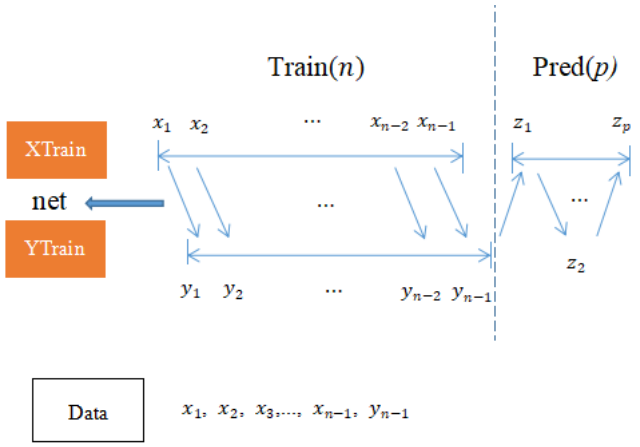

Fig. 9 Train and multi-step prediction of LSTM neural network

In this study, we use dynamic approach that update the model from the prediction value and use the concept of "delay" mentioned in NAR-ANN to transform the LSTM network. In Fig. 9, a "sequence to

sequence" is constructed in the training part for univariate prediction and it alternated the data set by one time step into XTrain and YTrain. And now it use the current time(t-1), as well as prior times (t-1),(t-2),(t-3),...,(t-9),(t-10) to predict the value at the next time instead of just using the value in the sequence(t-1) as Fig. 9 shown. For example, XTrain is $[[1\ 2\ 3\ 4\ 5\ 6\ 7\ 8\ 9\ 10]\ [2\ 3\ 4\ 5\ 6\ 7\ 8\ 9\ 10\ 11]]$, and the YTrain is $[[11]\ [12]]$.Use the last step of training to predict the first predicted value. Then rolling prediction is used to make multi-step prediction. So like every prediction method that use rolling prediction, it also will accumulate the error.

Table 2. Parameters applied in LSTM prediction model

Parameters	Value
Layer	3
Neurons per layer	300
Cost function	RMSE
Initial learn rate	0.001
Activation function	Sigmoid
MaxEpochs	1200
Time step	0.01s

Root Mean Square Error(RMSE) are used to evaluate the performance of the prediction model. In fact, we need to take the appropriate weight ω and bias b to minimize the loss function which is represented by RMSE. Because the process of training the model is the process of optimizing the cost function.

$$\mathrm{RMSE} = \sqrt{\frac{1}{\mathrm{N}}\sum_{i=1}^{N}\left(y^{(i)} - f\left(x^{i}\right)\right)^{2}} \tag{30}$$

Where N is the number of prediction data, $y^{(i)}$ is the true value, and $f(x^{i})$ is the prediction output. In fact, we need to take the appropriate weight ω and bias b to minimize RMSE. the lower RMSE values means better results.

SIMULATION RESULT

Table 3. Parameters applied in simulation

Parameters	Value
Density of the sea water (ρ)	1025 kg/m^3
Acceleration of gravity (g)	9.81 m/s^2
Radius (R)	5 m
Damping coefficient (C)	814000 kg/s
Stiffness (K)	78974 N/m
Buoy mass (m)	268344 kg
Added mass (m_∞)	134275 kg
Significant wave height (H_s)	4 m
Time step (dt)	0.01 s
Time prediction horizon (Δt)	3 s
Simulation time (t)	80 s

Regular waves

To verify the real-time control algorithm and prediction model, the dynamic model is compared in the case of control and no control. Valério(Valério, 2007) has revealed that aligning the peaks of WEC velocity and excitation force in irregular waves will improve the energy capture. Fig.10 has proved that the buoy is under the optimal control, the velocity of WEC is in phase with the excitation wave force, just like when resonance occurs, its energy is at its maximum. And the results obtained refer to 1 m amplitude incident waves.

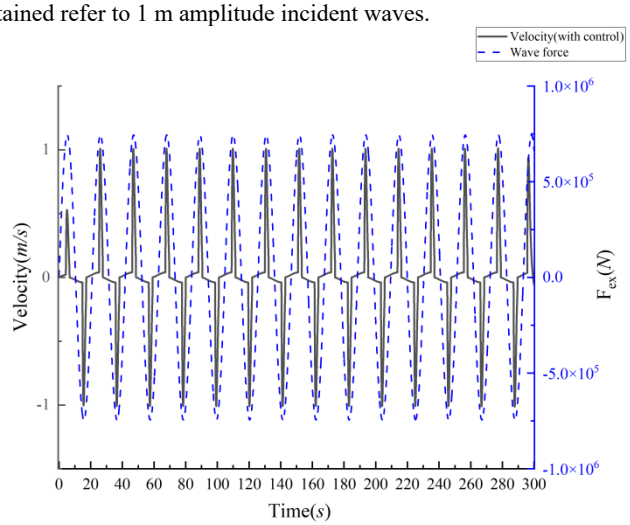

Fig.10 Phase between velocity and wave force in regular wave (ω = 0.3rad/s)

Irregular waves

If the device performs efficiently in regular waves over a frequency range, then it should be operate efficiently as well in irregular waves. Fig. 11 has shown the optimal control under the assumption that the excitation wave force is already known. From Fig. 11 we can see the wave force is more closely associated with velocity with control. It means that the velocity and the wave forces reach the maximum energy absorption with the real-time control. Because when the real-time control is implemented, the wave excitation forces mostly do positive work to buoy.

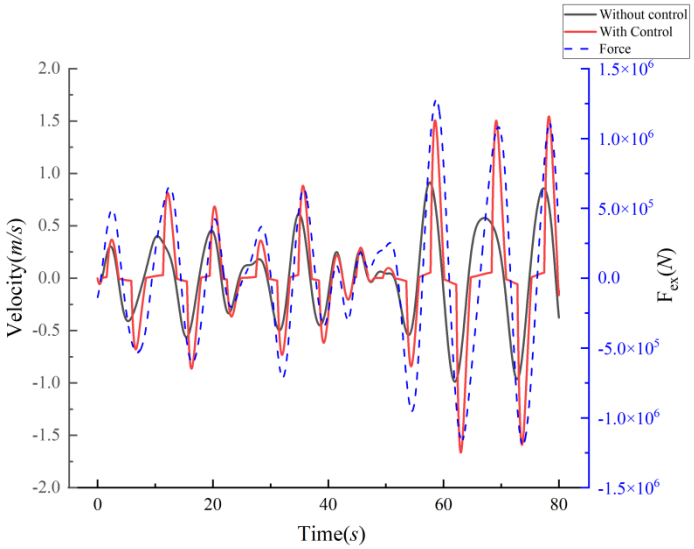

Fig. 11 Response of WEC based on optimal control

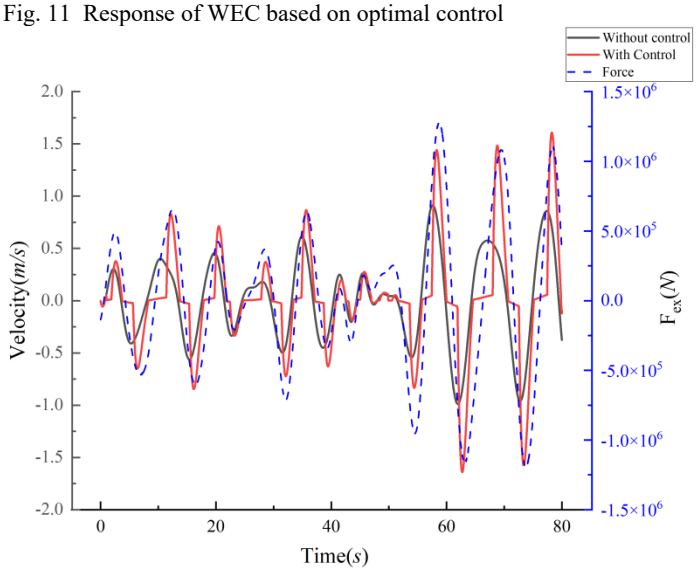

Fig. 12 Response of WEC based on NAR prediction model

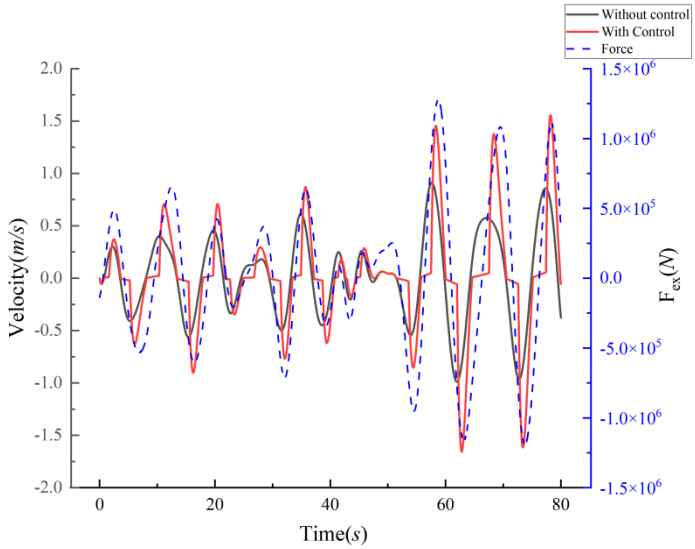

Fig. 13 Response of WEC based on NARx prediction model

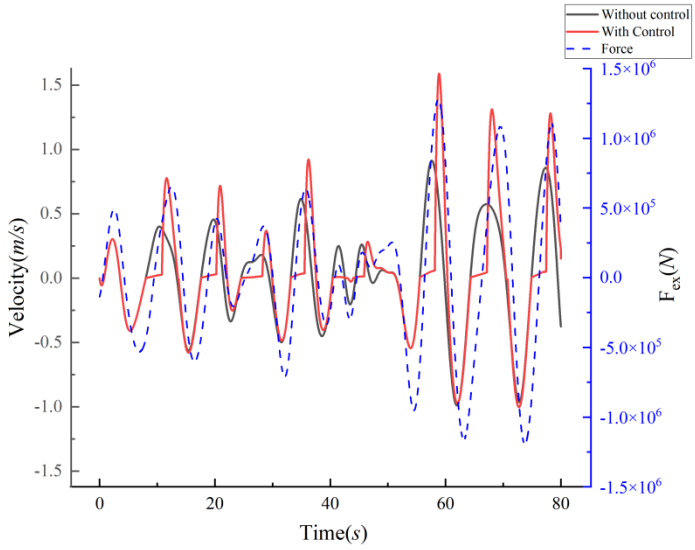

Fig. 14 Response of WEC based on LSTM prediction model

CONCLUSIONS

A real-time control of WECs Based on LSTM Artificial Neural Network is set up. Derived the value of optimal PTO control force to maximized the absorption of energy. Meanwhile, a reasonable prediction horizon is suggested. Simulation using MATLAB are conducted based on state-space model and wave excitation force data derived from Wadam, Sima, P-M wave spectrum. The numerical results show that optimal control strategy has a great performance improvement on power capture and the effect of sub-control based on types of prediction model is quite close to the optimal control. But due to the low data frequency and large time span of the wave excitation force itself, the prediction is not accurate enough. Compared with the single sequence (only the wave excitation force) in this paper, multi sequence prediction can ensure that there will not be too much deviation in prediction due to rolling prediction. Therefore, there is still room for progress in prediction of multi sequence.

ACKNOWLEDGEMENTS

This study was fully supported by the National Natural Science Foundation of China (Grant No.51979131) and China Scholarship Council Foundation (CSC201806680085). Technical assistances from Mr. Ming Zhang and Mr. Shuang-rui Yu (Ph.D. students) and Dr. Zhi-ming Yuan financial assistance are greatly appreciated.

REFERENCES

A. Babarit, A.H. Clement(2006), Optimal latching control of a wave energy device in regular and irregular waves, *Applied Ocean Research* 28(2)77-91.

Anderlini E,Forehand D,Bannon E (2017), et al. Reactive Control of a Wave Energy Converter using Artificial Neural Networks[J]. *International Journal of Marine Energy*, 19:207-220.

Budal K., Falnes J.(1980), Interacting point absorbers with controlled motion, 'in' Power from sea waves, Academic Press, 381-399.

Cummins,W.E. (1962). The impulse response function and ship motions[J]. Schiffstechnik, 1962, 9:101-109.

Dias, F, Ghidaglia, J-M, and Le Coq, G (2007). "On the Fluid Dynamics Models for Sloshing," *Proc 17th Int Offshore and Polar Eng Conf*, Lisbon, ISOPE, 3, 1880–1888.

Graebel, WP (2007). *Advanced Fluid Mechanics,* Academic Press, 362.

Giorgi S, Davidson J, Ringwood (2015). Identification of Nonlinear Excitation Force Kernels Using Numerical Wave Tank Experiments[C]// 11th *European Wave and Tidal Energy Conference (EWTEC)*.

Henriques J(2016) , Gato L , Falco A F O , et al. Latching control of a floating oscillating-water-column wave energy converter[J]. *Renewable Energy*, 2016, 90:229-241.

Hochreiter, S., J.Schmidhuber,(1997). Long Short-Term Memory, *Neural Computation*,9(8):1735-1780

Hulme A.(1982).The wave forces acting on a floating hemisphere undergoing forced periodic oscillations[J].*Journal of Fluid Mechanics,*443.

Kheisin, DE (1992). "Dynamics of Ice Cover Interacting with Ocean and Atmosphere," *Int J Offshore and Polar Eng*, ISOPE, 3(1), 43-50.

Kim, CH (2008). *Nonlinear Waves and Offshore Structures*, World Scientific, 516.

Li L.,Z. Yuan,Y. Gao,(2018) Maximization of energy absorption for a wave energy converter using the deep machine learning. *Energy*,165(-):340-349.

Longuet-Higgins, MS, and Fox, MJH (1977). "Theory of the Almost Highest Wave: the Inner Solution," *J Fluid Mech*, 80, 721-741.

Ming Zhang, Zhi-Ming Yuan, Sai-Shuai Dai,Atilla Incecik(2020). Development of a Novel Wave-force Prediction Model based on Deep Machine Learning Algorithms. *International Ocean and Polar Engineering Conference*; International Society of Offshore and Polar Engineers.

Sparrow,EM(1980b)."Forced-Convection Heat Transfer..Protuberances," *Num Heat Transfer*, 12(2), 149-167.

Tom, R. W.Yeung. Experimental Confirmation of Nonlinear-Model-Predictive Control Applied Offline to a Permanent Magnet Linear Generator for Ocean-Wave Energy Conversion[J]. *IEEE Journal of Oceanic Engineering*, 2016, 41(2):281-295.

Ueda, Y, and Rashed, SMH (1990). "Modern Method of ... Offshore Structures," *Proc 1st Pacific/Asia Offshore Mech Symp*, Seoul, ISOPE, 3, 315-328.

Vicente P C , AFO Falcão, Justino P . Nonlinear Dynamics of a Floating Wave Energy Converter Reacting Against the Sea Bottom Through a Tight Mooring Cable[C]// ASME 2010 29th International Conference on Ocean, *Offshore and Arctic Engineering*. 2010.

Valério D,Beirão P,Sá da Costa J(2007). Optimisation of wave energy extraction with the Archimedes Wave Swing. *Ocean Eng* 2007;34(17-18):2330-44.

Zhong,Q., and Yeung, R. W.(2017). "An Efficient Convex Formulation for Model-Predictive Control on Wave-Energy Converters." *ASME. J. Offshore Mech. Arct*. Eng.140(3): 031901.